

MONITORING NOAA/AVHRR AND METEOSAT SHORTWAVE BANDS CALIBRATION AND INTER CALIBRATION OVER STABLE AREAS

Cabot F., Dedieu G. and P. Maisongrande

LERTS, Unité mixte CNES-CNRS, 18, Avenue Edouard Belin, 31055 TOULOUSE CEDEX, FRANCE

Abstract

Monitoring of the calibration of shortwave sensors onboard NOAA and METEOSAT satellites has been the topic of various studies, involving atmospheric scattering, ocean glitter or the monitoring of radiometrically stable targets. Nevertheless, most of the developed methods, principally those based on desertic areas, suffer diverse constraints, particularly the need for reproducible geometric conditions. These requirements limit the possibility of a continuous monitoring of the gain drift of these instruments.

The method that we developed to achieve this aim relies on the difference in the frequency of all the phenomena that contribute to the measured signal. Atmospheric effects present strong daily variations superimposed on seasonal evolution. Directional effects depend on orbital characteristics of the platform, instrumental characteristics and also on the season. At last, one can assume that the temporal evolution of the calibration of the instruments does not present any cyclical behavior and obey a continuous law. These considerations led us to develop a method coupling models describing atmospheric and directional effects. This method is particularly adapted to the monitoring of the calibration over long term period, using desertic stable areas. The model parameters are prescribed from ancillary data sets (e.g. atmospheric water vapor content) or fitted with satellite measurements.

This method has been applied to several years of NOAA/AVHRR and METEOSAT measurements over several sites, considering each sensor separately in a first time and then altogether to attempt inter calibration of the two sensors.

1. INTRODUCTION

Throughout the last years, growing consideration has been given, in use of remote sensing data, to absolute calibration problems and gain drift monitoring. Although most of the satellites bear on board calibration devices, their use, especially in shortwave bands, remains difficult because of their uncontrolled ageing.

In order to solve such a problem, some experiments are periodically held to quantify the decaying of the sensors and to get a realistic gain value. These experiments suffer of low repeatability (presently one is held every 6 months approximately), atmospheric contamination, directional effects and of the very few sites being used.

The atmospheric and directional effects that influence the signal are difficult to take into account and the variations due effectively to the gain drift are generally of the same order of magnitude. The only difference in the behaviors of all these effects is their time period. Atmospheric effects present a yearly repeatability with strong random daily variations, effects of the non-lambertian behavior of the surface are ruled by the orbit repeatability and season whereas gain drift is expected to follow quite smooth variations with no repeatability all along the satellite life.

The method presented here takes advantage of these remarks, and is aimed at separating the variations according to their time period, and when possible, correcting them to isolate the variations due to gain drift. Our objective is to continuously monitor the variation of the gain of the sensors using large homogeneous areas as targets. Several sites have been selected and observed through 4 years. Their bidirectional behavior has been studied as well as their temporal stability. Some of these targets seem appropriate and experiments with several satellites were held. An attempt to complete an intercalibration of the different sensors used was also made.

2. DATA SET

The data set we used was extracted from the Global Vegetation Index product provided by the National Oceanic and Atmospheric Administration (Kidwell 1990). This archive includes, since 1985, digital count for visible and near infrared channels, brightness temperatures for thermal channels 4 and 5 and geometric conditions for NOAA/AVHRR satellites, subsampled to a spatial resolution of 16 km on a weekly basis. We choose to focus on NOAA/AVHRR-11, launched in September 1988 and still in operation at this day.

We selected 7 steady sites (Table 1), expected to be unvarying seasonally as well as from year to year.

Table 1 - Positions of the targets

	Latitude	Longitude	Surface type
Argentina	37.0 S	66.0 W	Prairie
Australia	20.0 S	132.0 E	Sand desert
Brazil	0.0	59.0 W	Forest
China	40.0 N	85.0 E	Sand desert
Kalahari	23.6 S	24.0 E	Stone desert
Libya	24.3 N	13.0 E	Sand desert
USA	32.5 N	106.2 W	Sand desert

The signal extracted from the original GVI product was calibrated in visible and near infrared reflectances, using the first post-launch available coefficients (from Kaufman and Holben, 1993) and correction for atmospheric effects where applied using the SMAC method (Rahman and Dedieu, 1994) with climatological values for water vapor (Oort, 1983) and ozone content (London *et al.*, 1976) and a constant aerosol optical depth of 0.05 at 550 nm. Surface temperature was derived through a split window formula (Kerr *et al.*, 1993). The mean and standard deviation of those three values were also computed over 3x3 pixel windows around selected target. These last quantities were used to filter the signal according to a method described in Cabot and Dedieu 1993a.

It can be seen on figure 1 that the signal we obtain after all these preprocessing is much smoother than the original signal but still shows variations of about 10%, partly due to bidirectional effects.

METEOSAT measurements were extracted from the so-called ISCCP B2 archive, which provide visible and thermal infrared channel digital counts from the METEOSAT satellites, subsampled to a spatial resolution of 30 km. One image is available every 3 hours. We focused here on METEOSAT-4, which entered in operation in June 1989 and is still in operation. Digital counts were extracted from this data set over the libyan desert, for two hours (11.30 and 14.30 UT), calibrated in reflectances using a fixed value of the calibration factor (Kriebel and Amann, 1991), corrected for atmospheric effects, in the same way as NOAA/AVHRR measurements, and filtered for cloud and large optical depth contamination. The filtering procedure is described in Dedieu 1993. Filtered reflectances, plotted on figure 2, still show a large dispersion, but are principally organized in two main clusters corresponding to the two hours of acquisition.

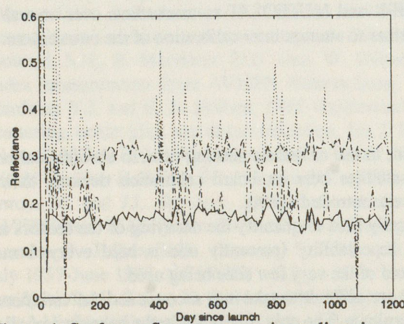


Figure 1. Surface reflectance over Australian site.

VIS: - unfiltered - filtered, NIR: .. unfiltered -- filtered

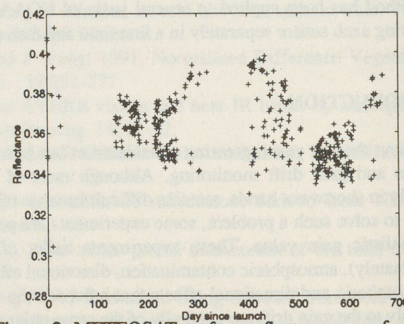


Figure 2. METEOSAT surface reflectance as a function of the number of day since launch, over Libyan desert.

3. METHOD

3.1 Gain drift monitoring

After accounting for atmospheric contamination, one has to consider bidirectional effects. In this study, Rahman *et al.* (1993) model was used. The basic assumption is that, if we are able to normalize the reflectances acquired throughout the whole period to a reference geometry, since this reflectance should be constant, we should see in this normalized signal only an evolution due to the gain drift of the instrument.

In order to achieve this normalization, we retrieved, through a least square computation, parameters of the model, performing the inversion on a sliding window. With these retrieved parameters, we computed reflectances for a reference geometry (Sun at zenith and nadir viewing). Since the reflectance of the surface is assumed to be constant, and according to the following expression for the reflectance:

$$\rho = \frac{\pi \alpha (DN - DN_0)}{E_0 \cos \theta_s (d_0/d)^2} \quad (1)$$

where ρ is the surface reflectance, α the gain of the sensor, DN the digital number, DN_0 the offset, E_0 the atmospheric solar irradiance at the sensor, θ_s the solar zenith angle, d_0 the distance between the sensor and the surface, and d the distance between the sensor and the surface. We assumed that the offset is constant. If we compute a reflectance ρ for a given target, we then can write:

where (0) represents the reference geometry. The procedure to the two sensors is the same. We assumed that the offset is constant. If we compute a reflectance ρ for a given target, we then can write:

3.2 Inter calibration

To achieve intercalibration, we used the same procedure as for the calibration of the reflectances. This is done by comparing the 1991, in a METEOSAT simulated digital counts.

where α_1 , α_2 and α_m represent the weights of the calibration factors, E_{01} , E_{02} and E_0 are the atmospheric solar irradiance at the sensor, θ_{s1} , θ_{s2} and θ_s are the solar zenith angles, d_{01} , d_{02} and d_0 are the distances between the sensor and the surface, and d_1 , d_2 and d are the distances between the sensor and the surface.

4. RESULTS AND DISCUSSION

In what follows, we compare the results of the calibration of the ratio of the calibration factors of the day of the year. We used a calibrated spectro-radiometer operated in order to get the ground truth transformed in satellite digital counts. In 1991, a desertic area in New Mexico (geometric conditions. iii) was used for measurements, corrected for atmospheric effects, sensor with calibration parameters for Arizona (UAZ).

4.1 Gain drift monitoring

The different sites, even if they are present in almost all the years, are not the same. Second, some of the sites have a remaining noise due to the atmosphere over the variations. We can see on the graphs (Fig. 1 and 2) shortly after the eruption of the volcano. Comparison between the results with the highest reflectance and the lowest reflectance they show very similar

where ρ is the surface reflectance, DN is the digital count as could be measured by the satellite, E_0 represents the exo-atmospheric solar irradiance in the considered wavelength band, d/d_0 the ratio of the distance Earth-Sun to the mean distance, α the gain of the sensor and DN_0 the offset of the sensor. All this procedure relies on the underlying assumptions that i) atmospheric corrections allow to overcome completely the effect of the atmosphere and ii) the variations of the calibration factor remain small enough to consider atmospheric effects as linear.

If we compute a reflectance in a reference geometry, simulate equivalent digital counts using first day calibration factor, we then can write:

$$\frac{\alpha(J)}{\alpha(0)} = \frac{DN(0) - DN_0}{DN(J) - DN_0} \quad (2)$$

where (0) represents the value of any parameter on the launching day and (J) the value at day J. We applied this procedure to the two sensors independently, AVHRR channels 1 and 2 and METEOSAT shortwaves.

We assumed that the offset of the AVHRR was constant throughout the period since there is no way to retrieve it from the GVI data. Kaufman and Holben (1993) estimated offset change from 41.0 to 33.9 between launching date and September 1990.

3.2 Inter calibration

To achieve intercalibration, we have to be able to make comparable the AVHRR reflectances and METEOSAT reflectances. This is done by combining the AVHRR visible and near infrared reflectances, according to Arino *et al.*, 1991, in a METEOSAT equivalent reflectance. After we computed normalized reflectances for the two sensors, and simulated digital counts, we then can write:

$$\alpha_M = \frac{E_0}{DN} \left[a_1 \frac{\alpha_1 (DN_1 - DN_0)}{E_{01}} + a_2 \frac{\alpha_2 (DN_2 - DN_0)}{E_{02}} \right] \quad (3)$$

where α_1 , α_2 and α_M represent the calibration factor for AVHRR channels 1 and 2, assumed perfect, and METEOSAT, a_1 and a_2 are the weights to apply to the AVHRR reflectances and depending on the spectral responses of the two sensors, E_{01} , E_{02} and E_0 are the exo-atmospheric solar irradiance for AVHRR channel 1 and 2 and METEOSAT, DN_1 , DN_2 and DN are the computed digital counts for AVHRR channels 1 and 2 and METEOSAT respectively.

4. RESULTS AND DISCUSSION

In what follows, we compared our results with those of various authors. But since we have no way to retrieve an absolute value for the calibration factor, the comparison is done only in term of drift, that is, we compared the temporal evolution of the ratio of the calibration factor at day J and calibration factor at day 0. For each author, we used for factor at day 0 the factor of the day of the first calibration experiment held after launch. The different sources are: i) Abel *et al.*, 1993, used a calibrated spectroradiometer flown over White Sands, New Mexico, which is our USA site. The radiometer was operated in order to get the same viewing and illumination geometry as NOAA-AVHRR, computed scene radiance was transformed in satellite level radiance using the LOWTRAN-7 code. ii) Kaufman and Holben, 1993, monitored twice a year a desertic area in North Africa, assuming its reflectance remains stable, and paying particular attention to matching geometric conditions. iii) Che *et al.*, 1991, also used the White Sands site but derived surface reflectance from SPOT measurements, corrected for atmospheric contamination. They present two sets of results obtained by calibrating SPOT sensor with calibration parameters given by French Centre National d'Etudes Spatiales (CNES) and by the University of Arizona (UAZ).

4.1 Gain drift monitoring

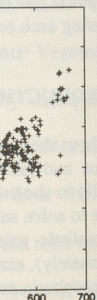
The different sites, even if they show very different evolutions of the gain, exhibit some general features which are present in almost all the results (Figure 3). First, the amplitude of the variations falls within the range observed by other authors. Second, some of the sites show a cyclical behavior. Whether this cycle is really a characteristic of the sensor or a remaining noise due to atmosphere is hard to decide, principally because of the lack of information regarding the atmosphere over the various sites. Over certain sites, such as USA, this cycle is annual and the most important feature we can see on the graphs (Figure 4). On this site, we can also notice the sharp diverging at the end of the period, starting shortly after the eruption of Mt Pinatubo. At last certain sites, such as Libyan desert, show good agreement at the beginning of the period but tend to diverge towards the end (Figure 5).

Comparison between the different sites was also done and particularly between China and Libya, which are the two sites with the highest reflectances. The calibration factor drift of these two sites is plotted on figure 6, and it is obvious that they show very similar behavior. When examining these results, one should keep in mind that these two sites are very

nces, using the first
meric effects where
vapor (Oort, 1983)
ce temperature was
e three values were
to filter the signal

n the original signal

visible and thermal
30 km. One image
1989 and is still in
30 and 14.30 UT,
1991), corrected for
large optical depth
figure 2, still show a
acquisition.



ce as a function
Libyan desert.

study, Rahman *et al.*
quired throughout the
is normalized signal

eters of the model,
ances for a reference
stant, and according

(1)

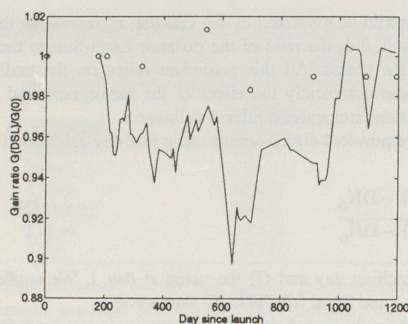


Figure 3.a Evolution of the calibration factor, as derived over Australia, for AVHRR channel 1. - This study. + Abel *et al.* o Kaufman and Holben x Che *et al* (CNES). * Che *et al.* (UAZ)

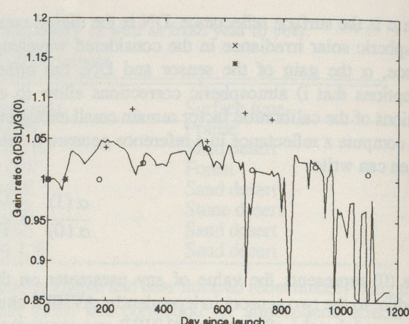


Figure 3.b same as figure 3.a, except over Brazil, for AVHRR channel 2

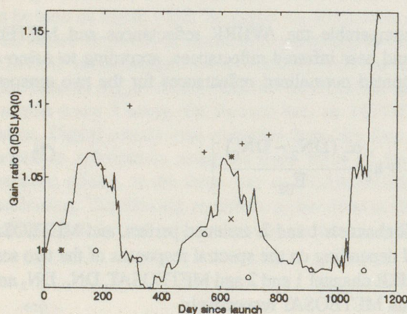


Figure 4 same as figure 3.a, except over USA

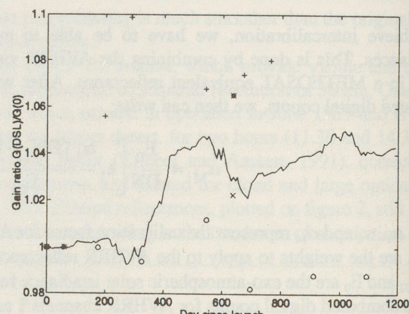


Figure 5 same as figure 3.a, except over Libya

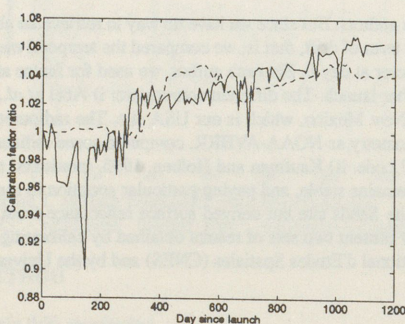


Figure 6.a Calibration factor ratio as derived over: - China and -- Libya, for AVHRR channel 1

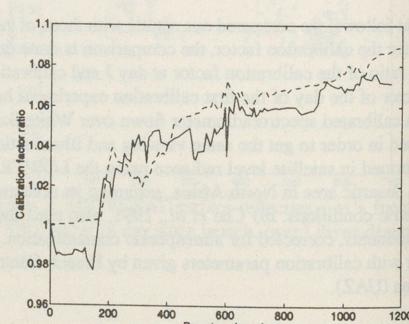


Figure 6.b Same as figure 6.a except for AVHRR channel 2

different in latitude, altitude, and climate.

The results obtained with METEOSAT show smoother evolution (Figure 7). In addition, they do not show any cyclical behavior as could be observed on the AVHRR calibration factor. It has to be underlined at this point that the two data sets widely differ in time resolution and that the GVI product suffers a subsampling, based on the maximization of vegetation index, particularly inadequate over desertic areas. Moreover, this subsampling is accompanied by a reduction in the angular sampling of the bidirectional reflectances that grieves the retrieval of consistent parameters. On the other hand, the angular sampling available in METEOSAT measurements is restricted in another way. Actually it presents only one view zenith angle.

Nonetheless, we tried to intercalibrate the two sensors using equation 3. The obtained values, plotted in figure 8, are larger than any calibration factor obtained elsewhere (Kriebel and Amann, 1993) but, at this time, we have no indication

on which sensor causes

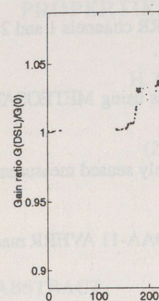


Figure 7 Evolution of the calibration factor over Libya, for METEOSAT

5. CONCLUSION

In this study we develop a method to correct the reflectances from the reflectances values. This work has outlined the need for a correction from the reflectances values. The correction is based on the reflectance due to this correction (atmosphere, directional, atmospheric effects using these various correction). This has been done over the world. There are always of the same differences appear on the reflectances: e.g. the atmospheric scattering is different. Still, the point that appears is that the directional behavior of the targets seem more appropriate for such areas. But the more the correction is applied, the more the calibration factor is affected. Still, the calibration factor is sensitive to atmospheric effects. After applying the correction, the intercalibration of the two sensors is about 30% higher. Despite all these uncertainties, the process is definite. The AVHRR data should lead to a better field of view sensors.

ACKNOWLEDGEMENTS

This work is supported by the Ministère de l'Enseignement Supérieur et de la Recherche.

on which sensor causes this effect.

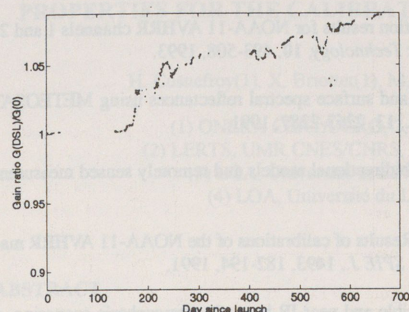


Figure 7 Evolution of the calibration factor, as derived over Libya, for METEOSAT

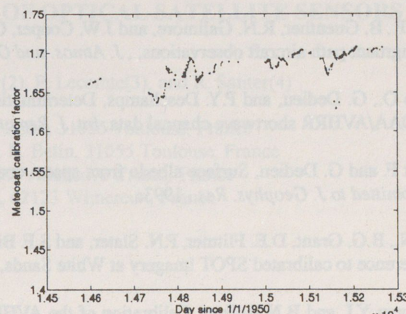


Figure 8 Calibration factor ($\text{W.m}^2.\text{sr}^{-1}.\mu\text{m}^{-1}/\text{DN}$), as derived over Libya, for METEOSAT, using AVHRR coefficient.

5. CONCLUSION

In this study we developed a method aimed at monitoring the evolution of the calibration factor of a sensor. This method relies on the analysis of long term series of reflectance measured over radiometrically stable areas. Though preliminary, this work has outlined that, if we are able to account for all the effects that perturbate the satellite signal, we can extract from the reflectances variations an information about the decaying of the sensor. Since the amplitude of the variation in reflectance due to this decaying is generally small, at least of the same amplitude as other perturbing effects (atmosphere, directional), it appears rather difficult to isolate what is due to the drift. The only difference that appears between all these effects being their time period, one has to take advantage of it. This was done by accounting for atmospheric effects using a climatology, supposed to remove from the signal the seasonal variations due to atmosphere, then by correcting directional effects, for which the period is both seasonal and short term (orbit repeatability). After these various corrections, the obtained signal can be used to derive the variations of the calibration factor of the sensor. This has been done over several sites, representative of various surfaces, latitudes and climates. The observed variations are always of the same amplitude as those observed by other authors, and show similar general behavior, even if large differences appear on certain sites. These discrepancies may be partly due to the large difference in the level of the reflectances: e.g. the Australian site reflectance is half worth the one of the Libyan site. Therefore, the contribution of the atmospheric scattering is more important, may induce more variability and hamper the retrieval of model parameters.

Still, the point that appears when evaluating the result of these computations is that this method allows to identify the directional behavior of the surface as well as the temporal evolution of the sensor. As it could be expected, brighter targets seem more appropriate for the application of this method since the effects of aerosol scattering is minimized over such areas. But the more important appears to be the homogeneity at a large scale of the selected targets. This allows to overcome misregistration problems and a more efficient filtering. The needed accuracy in all the preprocessings is such that it can hamper badly the retrieval of all the parameters and lead to rather large unaccuracy in the evolution of the calibration factor. Still, at this time, this accuracy is difficult to measure. It also appeared that, METEOSAT being less sensitive to atmospheric effects, the monitoring of its gain is easier.

After applying the described method to two different sensors (AVHRR and METEOSAT) we attempted the intercalibration of the two instruments. This could be achieved but lead to a calibration factor for METEOSAT visible channel about 30% higher than the one derived by other authors. At this time, and due to the lack of information related to the selected target, we can not decide from which step of the procedure this difference is due.

Despite all these uncertainties, the method appears able to derive consistent information useful in the normalization process. It is definite that a better knowledge of both the surface and the atmosphere, and daily, one km resolution, AVHRR data should lead to better results. These conclusions should be considered for the calibration of upcoming large field of view sensors.

ACKNOWLEDGEMENTS

This work is supported by the Programme National de Télédétection Spatiale, Région Midi-Pyrénées, CNES, CNRS and Ministère de l'Enseignement Supérieur et de la Recherche.

REFERENCES

- Abel P., B. Guenther, R.N. Galimore, and J.W. Cooper, Calibration results for NOAA-11 AVHRR channels 1 and 2 from congruent path aircraft observations, *J. Atmos. and Oceanic Technology*, **10**, 493-508, 1993.
- Arino O., G. Dedieu, and P.Y. Deschamps, Determination of land surface spectral reflectances using METEOSAT and NOAA/AVHRR shortwave channel data, *Int. J. Remote Sens.*, **13**, 2263-2287, 1991.
- Cabot F. and G. Dedieu, Surface albedo from space: coupling bidirectional models and remotely sensed measurements, *Submitted to J. Geophys. Res.*, 1993a.
- Che N., B.G. Grant, D.E. Flittner, P.N. Slater, and S.F. Biggar, Results of calibrations of the NOAA-11 AVHRR made by reference to calibrated SPOT imagery at White Sands, N.M., *SPIE J.*, **1493**, 182-194, 1991.
- Kaufman Y.J. and B.N. Holben, Calibration of the AVHRR visible and near-IR bands by atmospheric scattering, ocean glint and desert reflection, *Int. J. Remote Sensing*, **14**, 21-52, 1993.
- Kerr Y. and J.P. Lagouarde, On the derivation of land surface temperature from AVHRR data, *Proc. of the 4th AVHRR data users' meeting, Rothenburg, FRG*, 157-160, 1989.
- Kidwell K.B., Global Vegetation Index User's Guide, National Oceanic and Atmospheric Administration, World Weather Building, Washington, D.C., 1990.
- Kriebel K.T. and V. Amann, Absolute calibration of the METEOSAT-4 VIS-channel, *Proc. of the 8th METEOSAT scientific users' meeting. EUMETSAT publication P08*, pp. 33-38, Darmstadt, Germany, 1991.
- Kriebel K.T. and V. Amann, Vicarious calibration of the METEOSAT visible channel, *J. Atmos. and Oceanic Technology*, **10**, 225-232, 1993.
- London J., R.D. Bojkov, S. Oltzman, and J.I. Kelley, Atlas of the global distribution of total ozone July 1957-June 1967, *NCAR/TN-113+STR*, 1976.
- Oort A.H., Global atmospheric circulation statistics, 1958-1973, *NOAA Professional paper 14*, Rockville, Md., 1983.
- Rahman H., and G. Dedieu, SMAC: a simplified method for the atmospheric correction of satellite measurements in the solar spectrum, *Int. J. Remote Sensing*, In press.
- Rahman H., B. Pinty and M.M. Verstraete, A coupled surface-atmosphere (CSAR) model. Part 1: model description and inversion on synthetic data, *J. Geophys. Res.*, **98**, 20,779-20,789, 1993.
- Rahman H., M.M. Verstraete and B. Pinty, A coupled surface-atmosphere (CSAR) model. Part 2: Semi empirical model usable with NOAA Advanced Very High Resolution Radiometer data, *J. Geophys. Res.*, **98**, 20,791-20,801, 1993.

IN FIELD PROPERTIES

ABSTRACT

During a joint in-
desertic sites in AL
properties of the
measurements to d
near infrared and s
aims at the charac
airborne experimen
(AVHRR, Meteosa

1 - INTRODUCTION

Stable des
optical satellite sen
1990; Staylor, 199
Martinuzzi et al.,
such as POLDER
MISR/EOS (Diner
could be the assess

To investig
desertic zones in
multitemporal ser
stability of these si
next step is the me
averaged bidirectio
reflectance may be
angles θ_s and θ_v ,
limited in spectral
be supplemented
measurement cover

This paper
20 to March 21,
preselected by Co
characterize their
the TOA (Top Of
spatial and tempor
of meters to a fe
measurements suc
days and have bee
causes of spatial
qualitatively docu
patterns).